Realization and characterization of an XUV multilayer coating for attosecond pulses

Michele Suman,[2,*] Gianni Monaco,[1] Maria Guglielmina Pelizzo,[1,2] David L. Windt[3] and Piergiorgio Nicolosi,[1,2]

[1]*Information Engineering Department, University of Padova, via Gradenigo 6B, Padova, 35131 Italy*
[2]*National Research Council- National Institute for the Physics of the Matter, LUXOR Laboratory, via Gradenigo 6B, Padova, 35131 Italy*
[3]*Reflective X-ray Optics LLC, 1361 Amsterdam Ave., Suite 3B, New York, NY 10027, USA*
[*]*Corresponding author: sumanmic@dei.unipd.it*

Abstract: The experimental characterization of an aperiodic reflecting multilayer (ML) structure designed to reflect and compress attosecond pulses in the extreme ultraviolet spectral region is presented. The MLs are designed for the 75–105 eV spectral interval with suitable reflectance and phase behavior, in particular high total spectral reflectivity coupled with very wide bandwidth and spectral phase compensation. The experimental phase behavior of the multilayer has been obtained through electron photoemission signal using an innovative method that is presented and discussed in this paper. With this ML we have demonstrated pulse compression by reflection from 450 as to 130 as.

OCIS codes: (310.4165) Multilayer design; (320.5520) Pulse compression; (120.3940) Metrology; (120.5050) Phase measurement.

References and links

1. Y. Mairesse, A. de Bohan, L. J. Frasinski, H. Merdji, L. C. Dinu, P. Monchicourt, P. Breger, M. Kovačev, R. Taïeb, B. Carré, H. G. Muller, P. Agostini, and P. Salières, "Attosecond Synchronization of High-Harmonic Soft X-rays," Science **302**, 1540-1543 (2003).
2. R. Lopez-Martens, K. Varju, P. Johnsson, J. Mauritsson, Y. Mairesse, P. Salieres, M. B. Gaarde, K. J. Schafer, A. Persson, S. Svanberg, C.-G. Wahlstrom, and A. L'Huillier, "Amplitude and phase control of attosecond light pulses," Phys. Rev. Lett. **94**, 033001-1—4 (2005).
3. A. Wonisch, Th. Westerwalbesloh, W. Hachmann, and N. Kabachnik, "Aperiodic nanometer multilayer systems as optical key components for attosecond electron spectroscopy," Thin Solid Films **464–465**, 473–477 (2004).
4. A.-S. Morlens, P. Balcou, P. Zeitoun, C. Valentin, V. Laude, and S. Kazamias, "Compression of attosecond harmonic pulses by extreme-ultraviolet chirped mirrors," Opt. Lett. **30**, 1554–1556 (2005).
5. A.-S. Morlens, R. López-Martens, O. Boyko, P. Zeitoun, P. Balcou, K. Varjú, E. Gustafsson, T. Remetter, A. L'Huillier, S. Kazamias, J. Gautier, F. Delmotte, and M.-F. Ravet, "Design and characterization of extreme-ultraviolet broadband mirrors for attosecond science," Opt. Lett. **31**, 1558–1560 (2006).
6. A. Wonisch, U. Neuhusler, N. M. Kabachnik, T. Uphues, M. Uiberacker, V. Yakovlev, F. Krausz, M. Drescher, U. Kleineberg, and U. Heinzmann, "Design, fabrication, and analysis of chirped multilayer mirrors for reflection of extreme-ultraviolet attosecond pulses," Appl. Opt. **45**, 4147–4156 (2006).
7. M. Suman, F. Frassetto, P. Nicolosi, and M.-G. Pelizzo, "Design of a-periodic multilayer structures for attosecond pulses in the EUV," Appl. Opt. **46**, 8159-8169 (2007).
8. J. Lin, N. Weber, J. Maul, S. Hendel, K. Rott, M. Merke, G. Schoenhense, and U. Kleineberg, "At-wavelength inspection of sub-40 nm defects in extreme ultraviolet lithography mask blank by photoemission electron microscopy," Opt. Lett. **32**, 1875-1877 (2007).
9. A. Miyake, M. Amemiya, F. Masaki, and Y. Watanabe, "Phase measurement of reflection of EUV multilayer mirror using EUV standing waves," J. Vac. Sci. Technol. B **22**, 2970-2974 (2004).
10. E. Goulielmakis, V. S. Yakovlev, A. L. Cavalieri, M. Uiberacker, V. Pervak, A. Apolonski, R. Kienberger, U. Kleineberg, and F. Krausz, "Attosecond Control and Measurement: Lightwave Electronics," Science **317**, 769-775 (2007).
11. M. G. Pelizzo, M. Suman, G. Monaco, P. Nicolosi, and D. L. Windt, "High performance EUV ML structures insensitive to capping layer optical parameters," Opt. Express **16**, 15228-15237 (2008).
12. A. Aquila F. Salmassi, and E. Gullikson, "Metrologies for the phase characterization of attosecond extreme ultraviolet optics," Opt. Lett. **33**, 455-457 (2008).

#108948 - $15.00 USD Received 18 Mar 2009; revised 11 Apr 2009; accepted 20 Apr 2009; published 28 Apr 2009

13. S. Bajt, N. V. Edwardsb, T. E. Madeyc, "Properties of ultrathin films appropriate for optics capping layers exposed to high energy photon irradiation," Surf. Sci. Rep. **63,** 73–99 (2008).
14. M. E. Malinowski, C. Steinhaus, W. M. Clift, L.E. Klebanoff, S. Mrowka, and R. Soufli, "Controlling contamination in Mo/Si mutilayer mirrors by Si surface capping modifications," Proc. SPIE **4688**, 442-453 (2002).
15. D. L. Windt and W. K. Waskiewicz, "Multilayer facilities for EUV lithography," J. Vac. Sci. Technol. B **12**, 3826-3832 (1994).
16. S. Nannarone, F. Borgatti, A. DeLuisa, B.P. Doyle, G.C. Gazzadi, A. Giglia, P. Finetti, N. Mahne, L. Pasquali, M. Pedio, G. Selvaggi, G. Naletto, M.G. Pelizzo, and G. Tondello, "The BEAR beamline at Elettra," /AIP Conference Proc. **705**, 450 (2004).
17. S. Nannarone, A. Giglia, N. Mahne, A. De Luisa, B. Doyle, F. Borgatti, M. Pedio, L. Pasquali, G. Naletto, M. G. Pelizzo, and G. Tondello "BEAR a bending magnet for emission absorption and reflectivity," Notiziario neutroni e luce di sincrotrone **12**. 8-17 (2007).
18. http://www.elettra.trieste.it/experiments/beamlines/bear/
19. D. L. Windt, "IMD - Software for modeling the optical properties of multilayer films," Comp Phys **12**, 360-370 (1998).

1. Introduction

Generation of ultrashort light pulses, such as High Order Harmonics (HOH) generated by the interaction of laser with matter, has opened a new frontier in the physics of very short time scales. Manipulation of such pulses requires the use of optical components able to compress or preserve temporal duration. Ultrashort pulses can be generated in the interaction with gas jets of femtosecond laser pulses at high power density; the ionization of the atoms in the laser field produces a spectrum of laser harmonics extending up to the x-ray spectral region. It has been proven that HOHs are emitted in a time corresponding to a short fraction of the fundamental laser period; correspondingly, by suitably selecting a portion of the HOH spectrum a pulse with sub-femtosecond time duration can be obtained. In general harmonics have a phase mismatch characterized by a positive second order chirping [1]. In order to obtain a temporal compression of the attosecond pulses the harmonic phase mismatch has to be compensated. This goal has been obtained by Lopez-Martens et al. [2] using an aluminium filter, which is characterized by having a negative chirp in the 40-50 eV spectral region. Aluminium can be useful only in this spectral range, however, and so it must be replaced with other metallic materials in other spectral bands. In addition, the main drawback of using metallic filters to compress attosecond pulses is usually the strong absorption.

Chirped MLs give important advantages over the use of such filters: flexibility in phase compensation (thanks to realization of suitable designs according to the experiment); better focusing of the HOHs, since the focusing is performed through the ML optics itself in normal-incidence configuration, avoiding the grazing incidence configurations which are affected by large aberrations; and higher throughput, since their reflectivity is generally higher than filter transmission. MLs have therefore been proposed as a flexible solution that can be designed for optimum performance in different spectral bands [3]. MLs designed for attosecond pulse preservation/compression have aperiodic layers structures in order to achieve high reflectivity, very wide bandwidth, opportune harmonics phase correction and amplitude harmonic re-shaping. For example, Morlens et al. [4] have recently studied the second order constant chirping of the plateau harmonics phase in case that only the short electron quantum trajectories contribution is considered; this work demonstrates the possibility of compensating this chirping using an opportune broadband aperiodic ML in the 70–100 eV energy range. In a different work, Morlens et al. [5] have designed and characterized a broadband ML using a three-element structure in the 35–50 eV spectral range. Differently, Wonisch et al. [6] have designed and analyzed a broadband aperiodic ML characterized by a substantially linear phase to be applied to an isolated pulse in the cut-off region for temporal preservation. An innovative design for normal incidence chirped ML mirrors capable of reflecting pulses of approximately 130 attoseconds (as) duration by enhancing the reflectivity bandwidth and optimizing the phase-shift behaviour has been recently proposed [7]; moreover it has been demonstrated that these coatings would be less sensitive to deposition errors.

#108948 - $15.00 USD Received 18 Mar 2009; revised 11 Apr 2009; accepted 20 Apr 2009; published 28 Apr 2009

In order to completely characterize these unconventional aperiodic structures, it is necessary to adopt a technique that allows both reflectivity as well as phase recovery on top of the ML; in general full performance characterization of coatings realized for attophysics can be accomplished indirectly through very complex two colour photoionization experiments or through reconstruction of beating with interference of two-photon transitions [2,6]. When the EUV radiation interacts with a ML structure, the superposition of the incident and reflected electromagnetic wave generates a standing wave field distribution in the ML structure. Recently extreme ultraviolet (EUV) electron photoemission has been used to recover the EUV standing wave in order to test extreme ultraviolet lithography mask blanks [8] and to recover information on the phase shift on reflection [9]. The direct characterization of such coating by EUV standing wave analysis would allow a complete knowledge of the optics to be used in such experiments and would be a measurement directly related to the ML structure. It would be also a feedback for the deposition procedure [10]. The secondary electron photoemission spectroscopy allows to recover field intensity on top of the ML structure as function of energy (wavelength) and incidence angle [11]. Based on the same physical principle, an experimental characterization of broadband MLs with chirped phase has been performed by the used of Total Electron Yield signal [12].

In this work we present the realization of the ML proposed in Ref. [7] and its characterization through reflectivity and phase measurements. The experimental method followed in order to recover the phase from Total Emission Yield measurements and the results obtained are discussed. Differently from others, the TEY method proposed in this paper should have an important advantage: it should be insensitive to the materials irregularity present at the multilayer surface due to oxidation or hydrocarbon contamination on top of the ML (in particular, during the measurements performed in a synchrotron beamline, the exposure to EUV radiation of the sample in high vacuum condition can result in a change of the hydrocarbon layer morphology) [13,14]. The proposed method will overcome this problem by elaboration of TEY signals coming from the sample under test instead of using an external sample as a reference (e.g, a Si film), removing the error due to the different morphology of the two films. Furthermore, a second method is proposed in order to extend the measurements to regions of absorption edges.

The experimental results have then been used to verify the phase compensation of a Gaussian pulse with a spectral bandwidth of 30 eV and phase chirping 0.3 fs^2; then the outcome has been compared with the expected theoretical performances.

2. Multilayer design

An aperiodic multilayer coating having quadratic negative phase chirping for phase compensation of HOH spectrum coupled with broad band approximately rectangular reflectivity has been designed. The structure has been optimized to compensate for a Gaussian pulse with a bandwidth of 30 eV and a phase chirping of 0.3 fs^2; correspondently, a pulse of 450 as can be compressed to 130 as. Such a structure can reflect and synchronize the odd order harmonics spanning the range from 49th to 67th in the case of HOH generated by the interaction of a Ti:Sa laser with a gas jet. The coating has been optimized for s-polarized incident radiation. The design of this aperiodic structure is an optimization problem with many free parameters (i.e., the layer thicknesses) and consequently with a high computation complexity. For this purpose an optimization algorithm capable of exploring the domain of possible solutions (i.e. multilayer structures) has been implemented. The algorithm is able to acquire domain knowledge based on the values of a suitably defined merit function. During the optimization experimental aspects related to practical feasibility of the structure, as typical roughness and/or interdiffusion values at the interfaces are also taken into account; the interdiffusion and roughness has been simulated using the Nevot-Croce formalism in a two layer (a-Si/Mo) structure. Moreover the presence of a 1 nm native silicon oxide layer over the multilayer coating has been considered. Preliminary simulations show that hydrocarbon contamination results in a systematic shift in the multilayer phase behavior preserving the

#108948 - $15.00 USD Received 18 Mar 2009; revised 11 Apr 2009; accepted 20 Apr 2009; published 28 Apr 2009

reflectivity amplitudes. For this reason the presence of hydrocarbon contamination has not been considered during the optimization.

Due to the fact that all experimental aspects are taken into account, the algorithm focuses toward multilayer structures with high efficiency and stable performance, for which the layer thickness errors rising during the deposition process are not very critical, guaranteeing also the reproducibility in the realization of such structures.

The multilayer design and characteristics have been already presented [7]; here, to aid the reader, the layer thickness distribution from Ref. [7] is shown in Fig. 1. Such a ML structure, based on the alternation of Mo and a-Si layer materials, has been realized on a plane Si substrate by magnetron sputter deposition at RXO LLC [15].

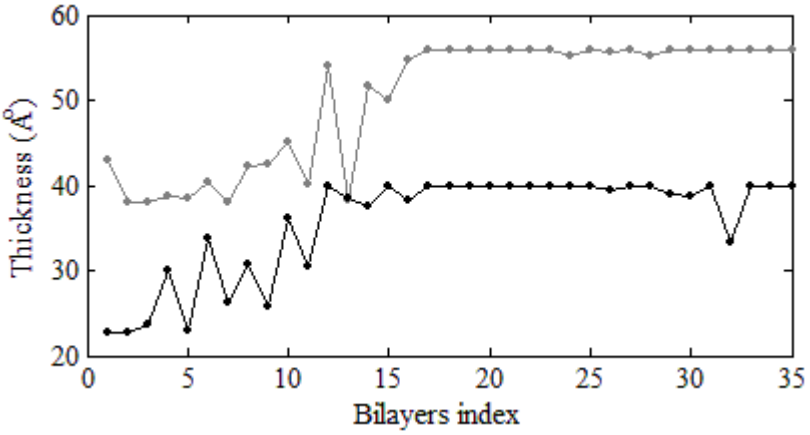

Fig. 1. In abscissa the progressive index period number starting from the top of the structure. The gray dots are the a-Si layers thickness while the dark dots the Mo ones. For the sake of clarity, points are joined with straight segments.

3. Multilayer phase characterization methods

The superimposition of the incoming and outgoing radiation creates a standing wave pattern in the multilayer structure, and this pattern is directly related to the multilayer phase. When extreme ultraviolet radiation impinges on the multilayer, electron photoemission is stimulated and it can be measured via total electron yield (TEY) data derived from drain current measurements on the sample. The TEY data is proportional to the standing wave pattern and consequently to the multilayer phase; this relation can be described by the following formula [12,9]:

$$TEY(E) = C(E) \cdot I_0 \cdot (1 + R(E) + 2 \cdot \sqrt{R(E)} \cdot \cos\phi(E)) \quad (1)$$

where C carries the materials dependence of the TEY data, I_0 is the intensity of the incident radiation, R is the reflectivity and Φ is the multilayer phase. In order to obtain the multilayer phase from the TEY signal the term $C(E)$ has to be determined. According to the method proposed by Aquila [12], the C term has been obtained using the TEY signal of a Si reference sample taking advantage of the negligible reflectivity signal of such a sample in the EUV spectral range. When either the multilayer or the silicon reference film are exposed to an air environment a non-compact carbon film and a silicon oxide layer (Fig. 2) are formed at the film surface. Precise thicknesses of these surface layers can be very difficult to determine; moreover, the consistence and thickness of the carbon layer varies over the whole sample area, resulting in a non-homogeneity of the surface. Finally, the carbon layer shows also a variation in time during measurement, due to its exposure to the EUV radiation in high vacuum conditions. Therefore, mixing the data obtained from the ML and the reference

#108948 - $15.00 USD Received 18 Mar 2009; revised 11 Apr 2009; accepted 20 Apr 2009; published 28 Apr 2009

sample can be critical due to different top layer morphology related to the different histories of the two samples.

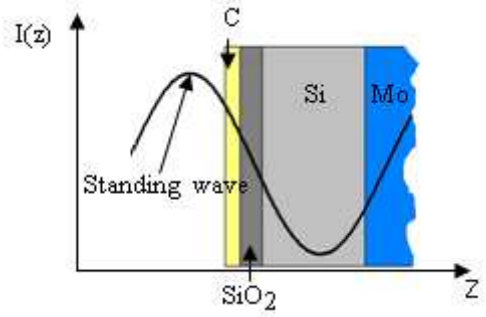

Fig. 2. Scheme of the top layers structure in a ML: the first layer is a very thin non compact carbon film, the second one is a silicon oxide layer and underneath the a-Si and Mo alternated layers.

Two new alternative methods, described below, are proposed in order to determine the term C in Eq. (1). Both methods are insensitive to the top layer morphology. The first method gives more accurate results, but it cannot be applied in the presence of an absorption edge; for this reason, in the restricted spectral region around the silicon absorption edge, our second method has been used (Fig. 3).

3.1 Method I

The TEY data have been detected at two different incidence angles: θ is the working incidence angle, while θ_1 is an angle slightly different from θ. According to the Bragg cosine law, the reflectivity signal measured at an incidence angle of θ at energy E_i and the signal measured at θ_1 at an energy E_{i+1} have the same value if the following relationship is true:

$$E_{i+1} = E_i \cdot \frac{\cos\theta}{\cos\theta_1}. \tag{2}$$

This approximation is valid for the spectral range considered, without absorption edges (see Fig. 3), and for a relatively small difference of incidence angles. In fact, if the angular difference between the two measurements is relatively small, the reflectivity curve shifts without any significant change of shape. However, this is not true for larger angle variations, since both the Bragg relation and the reflectivity change because of absorption and optical constants variations.

In this case, both reflectivity and phase (and therefore standing wave) assume the same values;

$$\begin{cases} R(E_{i+1},\theta_1) = R(E_i,\theta) \\ \phi(E_{i+1},\theta_1) = \phi(E_i,\theta) \end{cases}. \tag{3}$$

This concept is illustrated schematically in Fig. 4 in the case of a ML with a rectangular reflectivity.

#108948 - $15.00 USD Received 18 Mar 2009; revised 11 Apr 2009; accepted 20 Apr 2009; published 28 Apr 2009

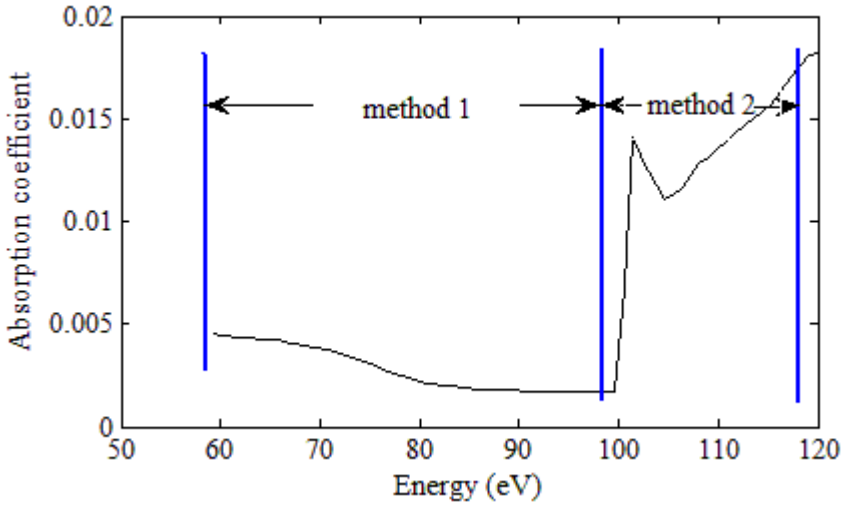

Fig. 3. In black, values of the imaginary part of the complex refractive index for the silicon material. The regions of application of method I and II respectively have been subdivided by grey continuous lines.

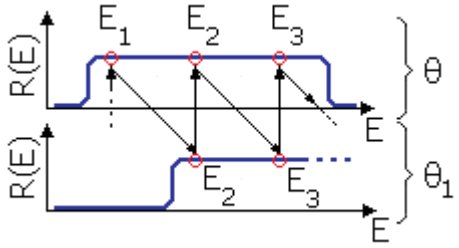

Fig. 4. Scheme of the concept express by the relationships (2) and (3) in the case of a rectangular reflectivity.

The ratio of the TEY signals Eq. (1) detected at two different incidence angles, θ and θ_1, and energies, E_i and E_{i+1}, related according to Eq. (2), is given by the following equation:

$$\frac{TEY(\theta_1, E_{i+1})}{TEY(\theta, E)} = \frac{C(E_{i+1})I_0(1+R(E_{i+1},\theta_1)+2\sqrt{R(E_{i+1},\theta_1)}\cos\phi(E_{i+1},\theta_1))}{C(E_i)I_0(1+R(E_i,\theta)+2\sqrt{R(E_i,\theta)}\cos\phi(E_i,\theta))}. \quad (4)$$

By the use of Eq. (3), this can be simplified as:

$$\frac{TEY(\theta_1, E_{i+1})}{TEY(\theta, E)} = \frac{C(E_{i+1})}{C(E_i)} = kost_i \quad (5)$$

In order to account for the different projected areas illuminated by the impinging radiation, the previous formula must be corrected by the ratio $cos(\theta)/cos(\theta_1)$:

$$C(E_{i+1}) = kost_i \cdot C(E_i) \cdot \frac{\cos(\theta)}{\cos(\theta_1)}. \quad (6)$$

Using a recursive application of this formula, it is possible to obtain the relative change of the C term versus energy, and the absolute value can be fixed by deducing C at least for one energy.

#108948 - $15.00 USD Received 18 Mar 2009; revised 11 Apr 2009; accepted 20 Apr 2009; published 28 Apr 2009

In Fig. 5 an experimental TEY signal derived at different energies is reported. The position of a minimum or a maximum of the signal corresponds to the node or anti-node of the standing wave distribution at the ML surface respectively; at those energies, therefore, the phase Φ assumes a value of π or 2·π.

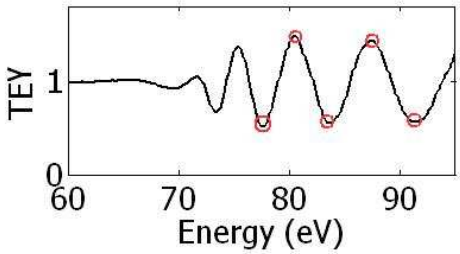

Fig. 5. Typical TEY signal; with red circle node and anti-node useful to determine the phase at correspondent energies.

3.2 Method II

The second method presented is a simplification of the first one. In this case, in fact, the incidence angle θ_1 is chosen in such a way that the ML has a negligible reflectivity in the whole ΔE spectral range considered:

$$R(\Delta E) \approx 0 \tag{7}$$

Generally θ_1 is quite different with respect to θ ($\theta_1 >> \theta$). Then Eq. (1) can be re-written as:

$$TEY(E,\theta_1) = C(E)\cdot I_0 \cdot (R + 2\cdot\sqrt{R}\cdot\cos\phi + 1) \cong C(E)\cdot I_0 ; \tag{8}$$

Therefore, the $C(E)$ term at incidence angle θ is given by:

$$C(E)\cdot I_0 = TEY(E,\theta_1)\cdot\frac{\cos\theta_1}{\cos\theta} \tag{9}$$

where the term ($\cos\theta_1/\cos\theta$) is again included as in Eq. (6).

4. Experimental results

Sample reflectivity has been measured immediately after deposition at RXO using a laser plasma source based facility; the sample also has been fully characterized 5 months after deposition at the BEAR beamline of the ELETTRA synchrotron [16-18]; the two sets of reflectivity data are in agreement, demonstrating the stability of the coating. In the experimental setup at BEAR the reflectivity has been measured by a detector photodiode and the Total Electron Yields (TEY) data has been collected by a Keithly 6517A current amplifier with a collection voltage of 20 Volt. I_0 is the intensity of the incident radiation (the incoming radiation intensity has been normalized to the ring current and therefore it is constant varying the energy values). A preliminary simulation of the effect on experimental outcome for reflectivity and phase behavior due to the polarization of incidence radiation has been performed. In fact, while the ML has been optimized for an s-polarized incident beam, the finite dimension of the exit slit in the synchrotron beamline does not allow the measurement using fully linearly polarized radiation. We changed the aperture of the entrance slit of the polarization selector placed at the beginning of the BEAR beamline, in order to take only the 4/11 milliradians of angular acceptance over and under the orbit, getting a polarization degree of I_{pol}=0.8. Reflectivity of the ML has been simulated by the use of IMD software [19], which is a point-and-click IDL application that can calculate specular optical functions of an arbitrary multilayer structure, i.e., a structure consisting of any number of layers of any thickness, and of any material, thanks to a

#108948 - $15.00 USD Received 18 Mar 2009; revised 11 Apr 2009; accepted 20 Apr 2009; published 28 Apr 2009

database of optical constants for over 150 materials. Reflectivity has been calculated assuming either fully s-polarized incident radiation (I_{pol}=1) or I_{pol}=0.8; the ratio between the curves obtained with the different polarization degrees are reported in Fig. 6. Above 80 eV the reflectivity measured with I_{pol}=0.8, is attenuated by a constant product factor; below 80 eV, the uncertainty in the polarization degree could lead to a maximum error of 2.5 % at 71.5 eV in reflectivity. On the contrary, phase is almost not affected by polarization degree uncertainty.

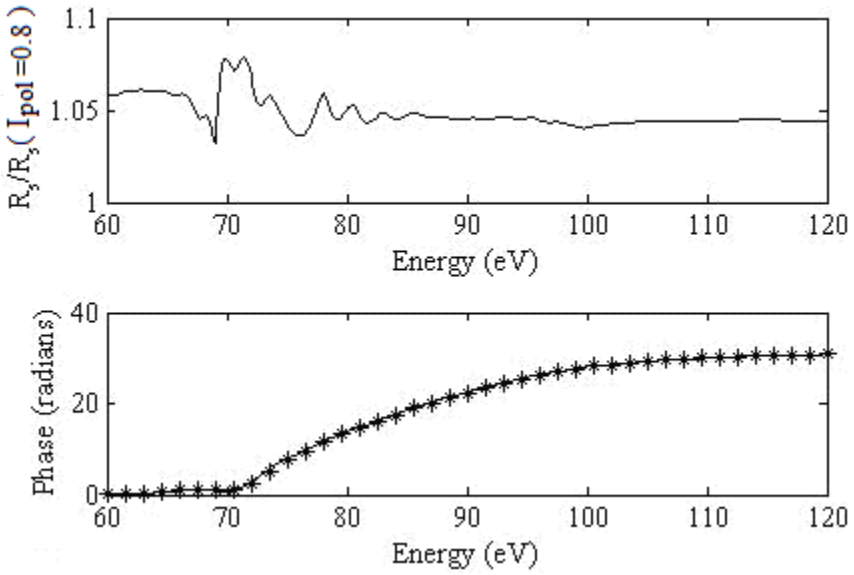

Fig. 6. Top figure: R(Ipol=1)/R(Ipol=0.8); bottom figure: Φs (continuos line) and Φp (star dots).

4.1 Reflectivity

Reflectivity measurements and theoretical expectations are reported in Fig. 7. The experimental data are shifted by a few eV relative to the calculation. This disparity is related to the experimental uncertainty in the Mo and Si deposition rates. As can be seen in the figure, the shape of the experimental curve follows quite well the theoretical curve. Interdiffusion and roughness at the interfaces can affect the reflectivity amplitude, systematically reducing the overall reflectivity. The polarization of the incident light is only minimally diminishing such curve as previously discussed. The effect of a thin carbon layer has been simulated, resulting in a negligible effect over reflectivity.

4.2 Phase recovering

Method I has been used to determined C(E) in the range 60-100 eV, while method II in the range 90-120 eV.

TEY experimental data have been used to recover cosΦ(E,θ), using Eq. (10) which has been derived directly from Eq. (1):

$$\cos\phi(E,\theta) = \frac{\dfrac{TEY}{C(E)\cdot I_0} - 1 - R}{2\cdot\sqrt{R}}. \qquad (10)$$

#108948 - $15.00 USD Received 18 Mar 2009; revised 11 Apr 2009; accepted 20 Apr 2009; published 28 Apr 2009

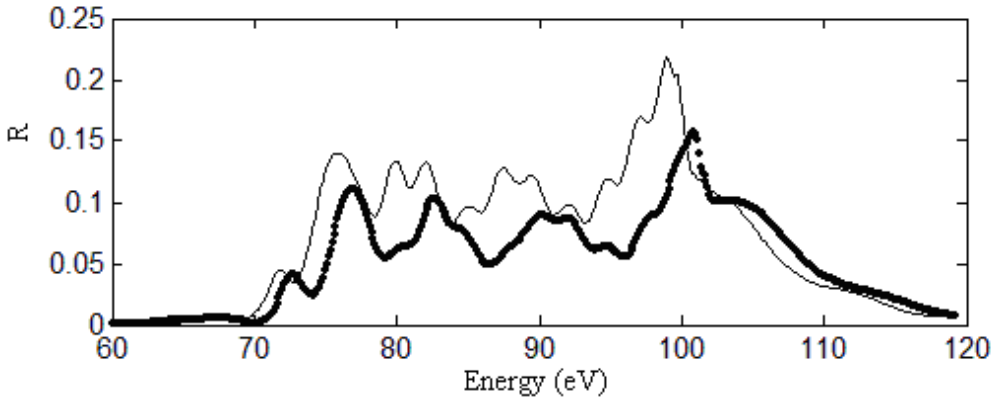

Fig. 7. Theoretical and experimental reflectivity.

The results are reported in Fig. 8 for the region 65-100 eV (method I). It can be seen that the experimental data (gray curve) at minimum never reaches the -1 value. This result can be explained in the following way: the TEY signal, in the present view, is assumed to depend only on the field at the multilayer surface; while this can be true in the case of the anti-node of the field at the surface, in the case of a node the very low TEY signal can have a significant relative contribution deriving from the field concentrated deeper in the ML structure. Consequently, the detected signal will deviate from the pure cosine behavior as close as the energy approaches a node position. For this reason, in order to reduce possible uncertainty in the method, the reference C(E) value has been derived at an anti-node position. In Fig. 8 a curve obtained by correcting the experimental values with a multiplicative factor is shown; the factor is linearly varying between 1.1 at the energies where $\cos\Phi(E,\theta)$ is minimum and 1 at the energies where $\cos\Phi(E,\theta)$ is maximum.

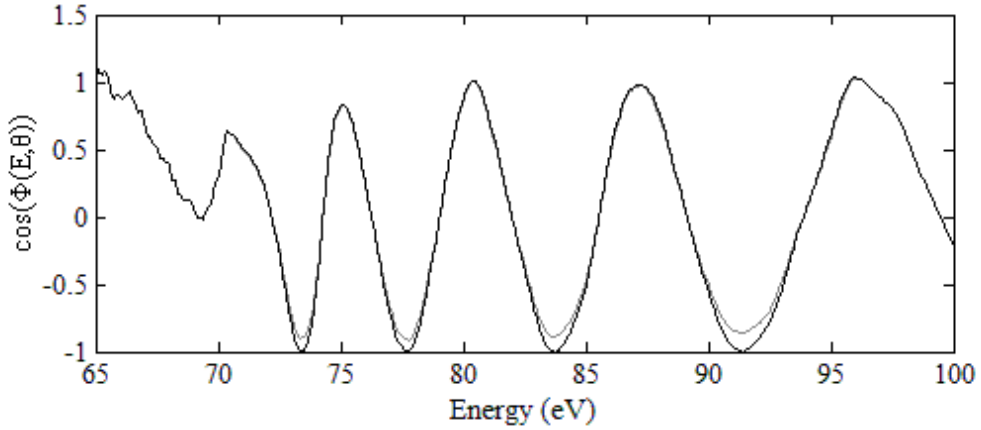

Fig. 8. Cosine of the phase experimentally derived by the TEY signal (in gray). Curve corrected at anti-node in black.

Finally, the phase recovered in the whole spectral range is reported in Fig. 9. Between 90 and 100 eV both methods have been used, showing a very good agreement in the overlapped spectral range, even though the second method is more noisy. The experimental phase has been fitted by varying parameters like interfacial roughness/interdiffusion and the thickness and optical constants of the Carbon layers. The results are difficult to interpret, however a roughness of 0.8 nm (as expected) could explain the observed shift.

#108948 - $15.00 USD Received 18 Mar 2009; revised 11 Apr 2009; accepted 20 Apr 2009; published 28 Apr 2009

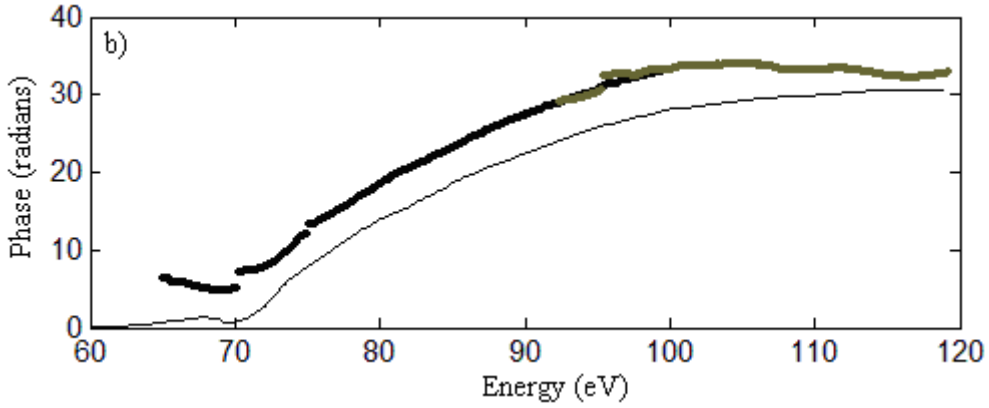

Fig. 9. Phase experimentally derived by the use of method I (black) and method II (grey). In continuous line the theoretical expected.

4.3 Gaussian pulse

The expected performance of the present structure can be derived from the reported experimental data. The reflected pulse has been computed both for the theoretically designed structure and for the actually deposited and characterized structure in the case of a Gaussian pulse with a spectral bandwidth of 30 eV and a phase chirping of 0.3 fs^2. The results are shown in Fig. 10 for the two samples and are normalized to the theoretical value. Both curves show the same time duration of about 130 as; a slightly lower (about 70%) peak of the intensity is present in the case of the deposited structure.

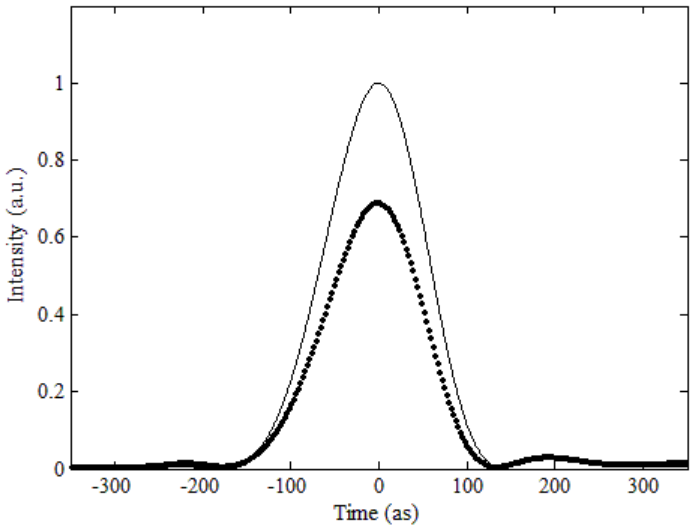

Fig. 10. Gaussian pulse with a spectral band of 30 eV and a phase chirping of 0.3 fs^2 as reflected by the theoretical ML and by the experimentally realized one.

5. Conclusions

An aperiodic Mo/a-Si multilayer for attosecond pulse reflection and compression has been realized. The multilayer has been tested for reflectivity and phase recovering in the whole spectral range of application. The phase has been recovered by the use of a method based on TEY signal measurement. The experimental data have been used to study the reflection of a

#108948 - $15.00 USD Received 18 Mar 2009; revised 11 Apr 2009; accepted 20 Apr 2009; published 28 Apr 2009

Gaussian pulse with a spectral band of 30 eV and a phase chirping of 0.3 fs^2. The resulting reflected pulse has the same time duration (about 130 as) as in the case of the theoretical ML, and an intensity peak reduced by about 30% with respect to the incident one. This result confirms the reliability and applicability of such multilayer optic designs in the manipulation of attosecond pulses.

Acknowledgments

This work has been supported by ASI grant n. I/015/07/0. The work has been performed also in the framework of the COST ACTION MP0601 "Short wavelength radiation sources". The authors acknowledge Angelo Giglia and Stefano Nannarone of BEAR beam-line for support during measurements at ELETTRA Synchrotron Trieste.

#108948 - $15.00 USD Received 18 Mar 2009; revised 11 Apr 2009; accepted 20 Apr 2009; published 28 Apr 2009